OPEN ACCESS

Effects of Trigger Method on Fire Propagation during the Thermal Runaway Process in Li-ion Batteries

To cite this article: Anudeep Mallarapu *et al* 2024 *J. Electrochem. Soc.* **171** 040514

Journal of The Electrochemical Society, 2024 **171** 040514

Effects of Trigger Method on Fire Propagation during the Thermal Runaway Process in Li-ion Batteries

Anudeep Mallarapu,[1,z] Nathaniel Sunderlin,[1] Vijayasekaran Boovaragavan,[2,*] Matthew Tamashiro,[2] Christina Peabody,[2] Thibault Pelloux-gervais,[2] Xin X. Li,[2] and Gregory Sizikov[2]

[1]*Center for Energy Conversion & Storage Systems, National Renewable Energy Laboratory, Golden, Colorado 80401, United States of America*
[2]*Google LLC, Mountain View, California 94043, United States of America*

Lithium-ion batteries are prone to fire hazards due to the possibility of thermal runaway propagation. During battery product development and subsequent safety tests for design validation and safety certification, the thermal runaway onset is triggered by various test methods such as nail penetration, thermal ramp, or external short circuit. This failure initiation method affects the amount of heat contributions and the composition of gas generations. This study compares two such trigger methods, external heating and using a thermally-activated internal short circuit device (ISCD). The effects of the trigger method on total heat generation are experimentally investigated within 18650 cylindrical cells at single cell level as well as at multiple cell configuration level. The severity of failure was observed to be worse for cells with ISCDs at single cell level, whereas quite the opposite results were observed at multiple cell configuration level. A preliminary numerical analysis was performed to better understand the battery safety performance with respect to thermal runaway trigger methods and heat transfer conditions.
 [DOI: 10.1149/1945-7111/ad3aae]

Manuscript submitted February 6, 2024; revised manuscript received March 19, 2024. Published April 12, 2024.

Supplementary material for this article is available online

Safety of Li-ion battery modules is extremely crucial due to the risk of thermal runaway and propagation of failure which can result in a catastrophic failure.[1] Thermal runaway is usually triggered when a cell reaches the onset temperature, usually 150 °C to 220 °C depending on the cell chemistry. Upon the onset of thermal runaway, a large amount of heat is released from the cell along with flammable and toxic gasses which can cause thermal runaway propagation in a multi-cell battery or ignite other flammable materials in proximity to the battery. The gasses generated during thermal runaway include hydrogen, carbon monoxide, carbon dioxide and hydrocarbons such as methane, ethane, and ethylene. Besides the dependency on the individual cell capacity and the number of cells in the battery module, the total amount of heat generated is a function of thermal runaway trigger method and how much of the initiating heat is transferred to the adjacent cells in a battery module.

Several test standards have been proposed to assess the safety of Li-ion batteries at cell, module, and pack levels.[2] In a real-world application, a battery failure can occur from (1) internal short circuit caused by internal defect or mechanical abuse (2) overcharging the battery that could occur from failure or lack of appropriate electrical protection (3) overheating the battery cells due to improper thermal management. During battery product development, the batteries are tested per several safety test standards to demonstrate the robustness of the product design and to obtain certifications from regulatory bodies. These tests simulate the failures that could occur: thermal abuse, mechanical abuse or electrical abuse and the test outcomes are carefully analyzed. For battery module level safety tests, demonstrating reduced probability of cell-to-cell thermal runaway propagation is of high importance. The most common method to initiate thermal runaway in the safety test methods is to use externally applied flexible thin film heaters to heat the cell external surfaces until thermal runaway occurs. The thermal runaway initiation method is specified in the test procedure such as UL9540a 4th edition, but since the initiation method may influence the outcome in terms of propagation this makes some of the test methods unrealistic. More understanding of the trigger method is required as it influences the final outcome of a battery safety test in the ability to contain the flames and sparks from escaping the module. This article focuses on this study which is a gap in the literature.

One of the current safety test standards, UL 9540 A, for evaluating thermal runaway fire propagation in battery energy storage systems uses external thin film heating on two adjacent cells to initiate thermal runaway.[3] Although the additional heat load could increase the overall extent of propagation, it is the preferred method of initiating thermal runaway due to the ease of application. But external heating of cells is unlikely to be representative of actual field failures because of the low probability of two adjacent cells in a module spontaneously going into thermal runaway under normal operating conditions. In an abuse condition, for example electrical abuse where the batteries are overcharged, it is possible for simultaneous cell thermal runaway initiation. Thermal runaway accidents typically occur due to an internal short circuit developing within the cell—either due to a manufacturing defect, dendritic growth or mechanical deformation resulting in separator failure.[4–6] Battery pack design strategies typically implement protection features at various levels (cell, module, system) to prevent simultaneous cell thermal runaway and propagation. Alternative failure initiation methods for testing purposes have been proposed[7,8] but comparison between these trigger methods is very limited within literature.

During an internal short circuit, electrochemical-thermal behavior has been studied using numerical models, and found to be non-uniform and influenced by factors including areal contact, the location and resistance of the short.[9–11] Ren et al.[12] found that joule heating from a short circuit is minimal compared to reaction heat during a thermal abuse test for a cell with $Li(NiCoMn)_{1/3}O_2$ cathode and graphite anode. Apart from severe internal short circuits, chemical crosstalk between the cathode and anode, can also play an important role in initiation of thermal runaway.[13] Reaction kinetics models have been developed to identify heat generation contributions from individual exothermic reactions within the battery.[14,15] Several studies have examined thermal runaway and propagation in pouch cells and cylindrical cells through a combination of experiments and simulations.[16–20] The effect of state of charge, capacity degradation, decomposition reactions and internal

*Electrochemical Society Member.
[z]E-mail: Anudeep.Mallarapu@nrel.gov

short circuits have also been studied.[21–23] Mechanical abuse induced short circuits are especially important for vehicle applications because crashworthiness is a crucial design objective. Xu and colleagues investigated the failure risk of batteries under mechanical deformation under various conditions along with comparison of fresh cell response to aged cells.[24–26] Safety response for cells during high velocity dynamic impact, and the resulting capacity loss of cell failure have also been experimentally characterized.[27,28] Cell venting during thermal runaway can result in release of toxic and flammable gasses that further assist cell-to cell propagation.[29,30] The complexity of thermal, mechanical, and electrochemical process interactions suggests that we cannot ignore the trigger method or failure initiation method when assessing the thermal propagation tolerance within a battery module design.

In this study, we experimentally compare the external thin film heating method to an alternative thermal runaway initiation method employing an Internal Short Circuit (ISC) device embedded in the initiating cell. During normal battery operation, internal short circuits can happen due to various reasons such as dendritic growth, internal defects, or mechanical abuse. ISC device is a useful tool to experimentally simulate such short circuits, but some initial heat is required to activate it. External heating can mimic failure of thermal management systems that leads to some cells getting overheated. External heating is also the failure mode experienced by the neighboring cells during thermal propagation. Even though the external heating causes a short circuit due to separator shrinkage, the magnitude of short circuit resistance varies widely while the ISC device produces more consistent results in terms of both thermal runaway initiation and short circuit resistance. The severity of failure was observed to be worse for ISC devices than thin film heating in single cell tests, but more limited propagation was observed for the ISC devices than the thin film heating in multi-cell test configurations.

Experiments

We performed tests using two different methods to trigger battery thermal runaway in both individual cell and multi-cell module configurations. The two methods are (A) external heating using a thin film heater attached to the cell, similar to the method commonly used in test methods and standards and (B) internal heating using an internal short circuit device.[31] The results from these two different trigger methods are compared and analyzed.

Method A is external heating, which involves wrapping the cell with a thin film heater (part number 30450DHT from the supplier: Phoenix Thermal Supply) and applying a constant heat generation rate to the cell until thermal runaway occurs. Method B uses a cell implanted with an ISC device and this cell is wrapped with an external heating pad. In this case the heating pad is used to activate the ISC device so less heat is added to the cell than in Method A. The self-heating from the internal short circuit causes the temperature increase resulting in thermal runaway. All tests were performed on18650 cylindrical cell with a capacity of 3.5 Ah and nominal voltage of 3.6 V.

The ISC device was developed in collaboration between NREL and NASA to simulate internal cell failures.[31] In a cell with an embedded ISC device, a short circuit can be induced by simply heating it to a modest (~60 °C) temperature. The ISC device consists of outermost layers with copper and aluminum discs which are directly in contact with the anode and cathode currently collectors respectively within a cell. A portion of the battery separator is cut out, and electrical insulation is instead provided by a wax layer with a melting temperature of approximately 60 °C. When the cell is heated the wax melts providing a current pathway (an electrical short circuit) between the electrodes. A copper puck rests within the stack of ISC as shown in Fig. 1 to ensure a good electrical contact between anode and cathode once the short circuit is induced. This method has been used to accurately control the location and timing of internal short circuits in analyzing thermal runaway initiation and propagation.[32]

A total of four test cases were carried out with two tests at cell level and two more tests at module level as summarized in Table I. All tests were carried out inside a closed chamber with no forced airflow and uncontrolled environment. The ambient temperatures were 14 °C–16 °C during single cell tests and 19 °C–22 °C for multicell tests. The heat generation and thermal propagation behaviors are recorded in each test case. All tests were performed with a target heating rate of ~ 6 °C/min for the film heaters. All the cells were fully charged to 4.1 V before the test, the cells are charged from the shipping SoC. During the single cell tests, cell voltage and temperatures at 3 locations (anode terminal, cathode terminal and cell center under heater pad) were monitored. For multiple cell configuration tests, all cells were electrically isolated from each other, and the cell temperatures were monitored using one thermocouple attached at the center of all the eight cells, the thermocouples on two trigger cells are located on top of the heater pad. Figure 2 shows the assembled multiple cell configuration within the cell holder that represents the battery module equivalent for this study, the thermocouple locations are also shown. Cells 4 and 5 are the trigger cells on which the thermal runaway initiation method is applied. No major heat conduction pathways exist between the cells, and hence most of the heat transfer between trigger cells and neighboring cells is convective and radiative.

Results and Discussion

Single cell tests.—The single cell tests show that the ISC implanted cell (Method B) reaches higher peak temperatures during thermal runaway than the cell with the external thin film heating method. Figure 3 shows the overall comparison of cell temperatures between both test methods, A and B. The temperature profiles during the initial heating through thermal runaway are plotted as a function of time. Also shown in Fig. 3 is the cell voltage profile during the test. The differences in temperature profiles from the three thermocouples indicates significant non-uniformity in the cell temperature profile during thermal runaway. For the case of ISC device method a total energy of around 5.923 kJ was supplied to the heater pad to cause thermal runaway. In case of external heating, this energy was much higher (around 17.480 kJ) as the heater was running for longer until cell surface temperature was close to 200 °C. Additionally, the time to thermal runaway initiation is much faster using the ISC device; the short circuit occurs about 550 s from the time the external heating started. Thermal runaway initiation occurs within 200 s of the internal short circuit, or a total of 700 s from the start of the experiment. For the external heating method, a short circuit forms around 500 s prior to the onset of thermal runaway, taking a total of 2200 s from the start of the experiment for the thermal runaway to occur.

The different methods also result in different voltage characteristics during the internal short circuit onset. The ISC device activation produces a much sharper voltage drop to near-zero compared to the short-circuit produced by external heating as shown in Fig. 3. The extent of voltage drop is determined by both the internal cell resistance and short-circuit resistance, however the short-circuit for these methods occurs at different temperatures (at ~ 120 °C in method A and ~57 °C in method B) that has an effect on the magnitude of internal cell resistance. The non-zero voltage in Method B indicates the electrochemical energy capacity stored in the cell is not fully drained which is evidenced from the voltage profile of Method A. The zoomed in cell voltage profiles are shown in Fig. 3 as inset plots, Method B shows non-zero voltage of about 250 mV while Method A showed absolute zero voltage prior to the occurrence of thermal runaway.

As seen in the inset plot of Fig. 3a, voltage oscillations might be arising as a result of electrolyte evaporation. Although the absolute value of voltage seems low, this could translate into a significant

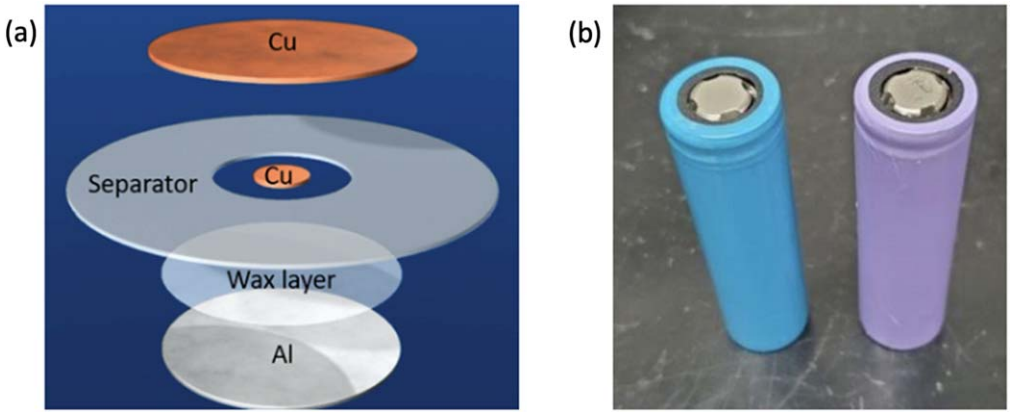

Figure 1. (a) Exploded view of Internal Short Circuit (ISC) device (b) Baseline Cell (left) and ISC implanted Cell (right).

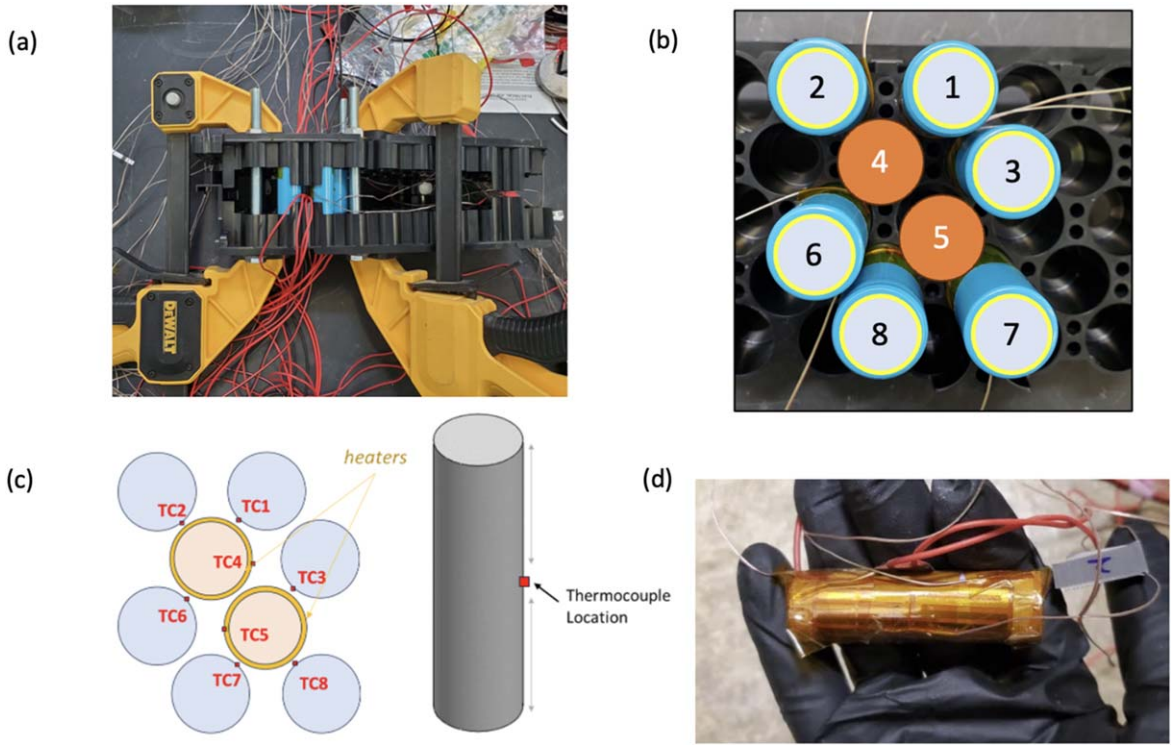

Figure 2. (a) Assembled module with clamp holder used to represent the equivalent module for this test objectives. (b) Configuration of cells for the representation of module level tests, cells 4 and 5 are the initiating cells triggered using either ISC or external thin film heating. (c) Thermocouple locations for multicell level tests. (d) Test setup for single cell level tests.

Table I. List of experimental tests performed.

#	Test details	Failure initiation method	Number of cells
1	Single Cell - Method A	External Heater Film Heater	1
2	Single Cell - Method B	Implanted ISC device activated using External heater	1
3	Multiple Cell Configuration - Method A	External Heater Film Heater	8 (2 cells triggered)
4	Multiple Cell Configuration - Method B	Implanted ISC device activated using External heater	8 (2 cells triggered)

amount of the cell full charge capacity due to the fact that the heating delaminates the internal layers and causes significant impedance rise. For Method A, thermal runaway occurs after the cell voltage reaches zero, around 200 s before thermal runaway. With test Method B (ISC device), the battery still has a remaining non-zero state-of-charge (SoC) as inferred from the non-zero cell voltage when thermal runaway initiation occurs, this additional stored energy in the cell results in the higher peak temperatures. The cell venting for Method A occurs before the thermal runaway while the venting and thermal runaway occurs at the same point of time in Method B. It should be noted that the cell voltage drop is caused by the discharge of electrochemical energy capacity. At around 1620 s voltage drop occurs in method A due to a short circuit formed by separator shrinkage. This is followed by voltage recovery due to the

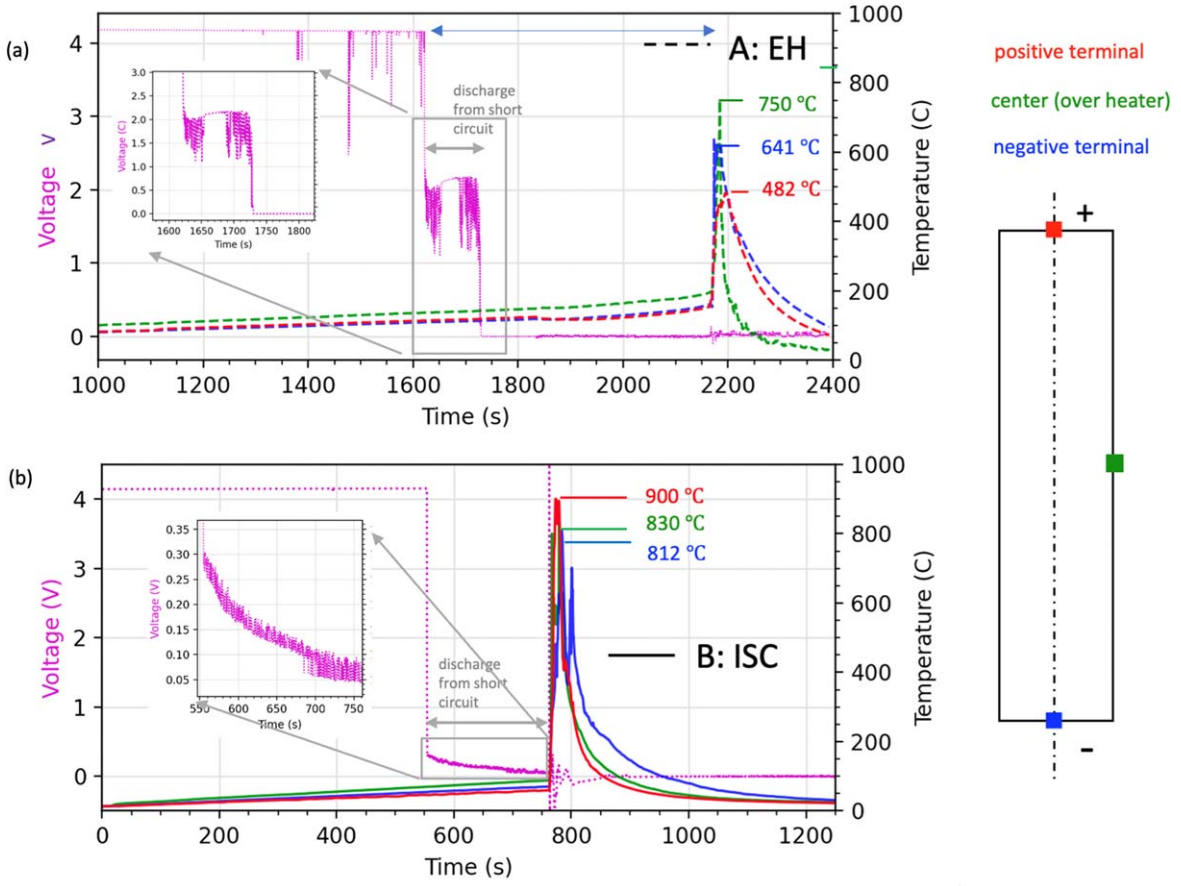

Figure 3. Comparison of temperatures between single cell test methods, A: External Heating (EH) and B: Internal Short Circuit (ISC) Device.

improved transport properties such as solid-phase diffusion and ionic conductivity at higher temperatures.[9] Decomposition would decrease the voltage further. As shown in Fig. 4, for the case of ISC implanted cells, thermal runaway process occurs for a longer duration as the exothermic reactions progressing from the center of the cell and quickly exhausted as it propagates further into the cell terminal ends.

As shown in Fig. 4, Method B with the ISC device actually results in higher peak temperatures than Method A which relies on the external heater to initiate thermal runaway; this seems counter-intuitive because the external heater adds significantly more heat to the cell in addition to the internal heating and exothermic reactions than the ISC device. This observation implies that the short circuit discharge and consequent joule heating is critical to the peak temperatures achieved in single cell thermal runaway. The additional heat from the internal short circuit discharge contributed to higher peak temperatures when using the ISC device, while less heat is generated by the short circuit discharge caused by the external heater (Method A) Cells being in a completely discharged state for Method A with external heating could also mean lower heat generation during the exothermic decomposition reactions, resulting in lower peak temperatures compared to Method B where the cells are at non-zero voltage when the thermal runaway occurs.

It should be noted that method A with external heating would have more ability to heat the negative electrode, as the heating is applied directly to the cell can which is electrically connected to Cu foil in anode. For method B, the cell receives localized heat generation from inside near the short circuit device. Overall greater peak temperatures in method B, indicate that the internal short circuit device produces higher rapid heat generation during thermal runaway. Apart from the effect of short circuit current, ISC device activation can also enable reaction between anode and cathode at a lower temperature compared to method A. During external heating (method A), the cell soaks for a long time (>10 mins) at an elevated temperature (>100 °C) before undergoing thermal runaway. Cell internal resistance can increase significantly at these temperatures which can lead to highly reduced short circuit joule heating when the separator fails. During this slow heating up time, even though there is onset of some exothermic reactions, the heat generation is countered by continuous heat loss from radiation and convection. This means increasing heating rates can increase the severity of external heating (method A) trigger method.

Tests with multiple cell configuration.—Figure 5 shows the overall comparison of temperature responses between Test # 3 and Test # 4 (refer Table I) for the experiments with multi-cell configurations consisting of eight cells. The eight thermocouples were placed at the center of each cell as shown in Fig. 2c and the temperature measurements from each cell is called as TC1: cell 1 center, TC2: cell 2 center,TC3: cell 4 center, TC4: trigger cell, thermocouple on top of the heater pad, TC5: trigger cell, thermocouple on top of the heater pad, TC6: cell 6 center, TC7: cell 7 center, TC8: cell 8 center. We noticed lower peak temperatures in the tests with multiple cell configurations compared to the single cell tests because some of the heat from the heater pad is transferred to the cell holders and adjacent cells.

Figure 5 shows that the highest peak temperatures are observed with external heating (Method A) compared to the ISC device in Method B. This observation is interesting as it is quite the opposite to our earlier findings in single cell-level tests as shown in Figs. 3 and 4. These results indicate that in multi-cell configurations, the external heating method produces an environment more amenable to cell-to-cell thermal runaway propagation than the ISC device method. This could be due to the additional heat required to force the triggering cells into thermal runaway and the incidental heating

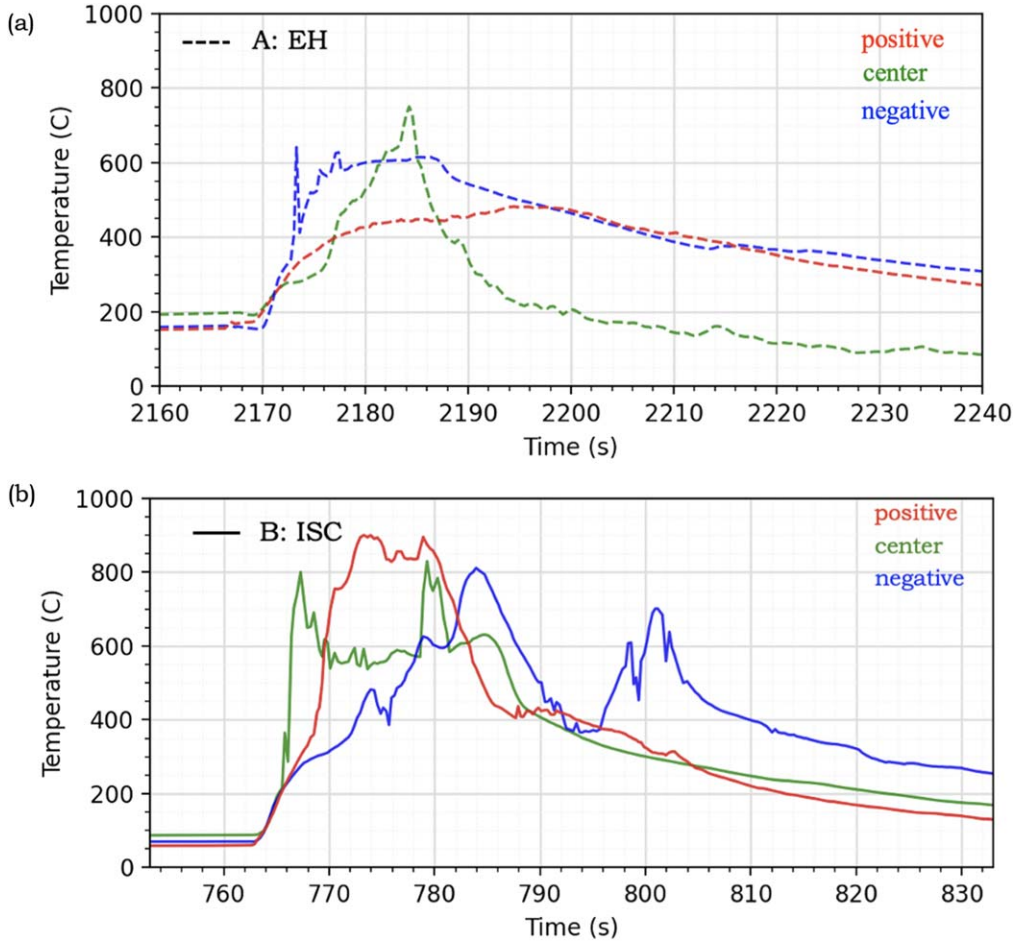

Figure 4. Comparison of temperate profiles between (a) Method A with external heating and (b) Method B with internal short-circuit device (ISC) from the single cell tests.

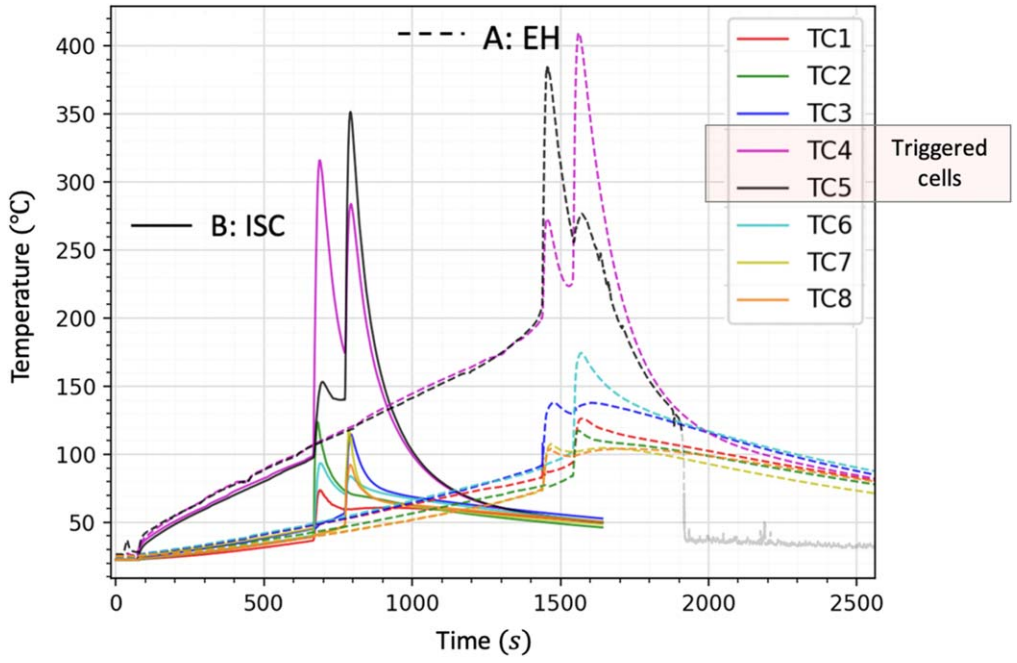

Figure 5. Comparison of temperatures between multicell level tests.

of adjacent cells which will then be closer to thermal runaway conditions when the trigger cells go into thermal runaway. In the case of Test #4 Method B with ISC devices, heating is required only to trigger the internal short circuit current that does not require excessive amount of heat as in Test #3 Method A but still require a little more heat than the case of single cell ISC Test #2 Method B. Although the trigger cells in Test #4 had non-zero voltages during the thermal runaway and the cell venting happens together with thermal runaway, these effects are not prominent as the severity of failure event depends on the heat transfer conditions around the trigger cells as well as the failure initiation methods.

From Fig. 5, it can be seen that temperature rise during thermal runaway is of similar magnitude for both methods, while it was clearly not the case in single cell tests (Fig. 4). This indicates that during multicell configuration tests, thermal runaway mechanism is similar between ISD activation and external heating. Further investigation required to understand precise conditions of the trigger cells during initiation of thermal runaway. At the multicell level, the major difference is additional thermal mass from the cell holder and the surrounding cells causing lower temperature peaks. These conditions can influence the rate of heat loss, consequently affecting the duration between internal short circuit and thermal runaway. The cell state of charge plays an important role in determining heat generation from exothermic reactions.[33] This again reiterates that the severity of failure depends on heat transfer conditions as well as the failure initiation method.

In Test #3 Method A, the heating rates of cells #4 and #5 were respectively 6.7 and 6.6 °C min^{-1}. Just as in Test #1, the minor inflections occurred in temperature plots of the trigger cells due to venting of hot gasses. Thermal runaway occurred in cell #5 first 22 min and 30 s after the start of external heating. At that moment, the adjacent cell temperatures ranged from 72 °C-90 °C. The heater for cell #4 switched off after the thermal runaway process initiated on the cell #5. Nevertheless, cell #4 entered thermal runaway approximately 100 s after cell #5. The maximum adjacent cell temperature during the test was 174.6 °C, on cell #6. Although this temperature level is within the vicinity of where the trigger cells ruptured and started smoking, the module cooled too quickly for any such event to manifest in cell #6. Thermal runaway did not propagate to any of the adjacent cells, and all adjacent cell voltages remained above 4.1 V after the test was complete. Test #4 Method B used two ISC-implanted cells as the trigger cells surrounded by six other cells. The quantity and placement of thermocouples are identical to Test #3. The heating rates of the cells averaged 6.2 and 6.3 °C min^{-1}. Cell #4 was the first to enter thermal runaway at almost exactly 100 °C, after heating for 9 min, 52 s. The peak adjacent cell temperature at that moment was 45 °C, on cell #3. The heater on Cell #5 was left on while cell #4 was in thermal runaway but it could not completely counteract the cell cooling even as cell #5 absorbed heat from cell #4. Roughly 100 s after cell #4, cell #5 entered thermal runaway. The peak adjacent cell temperature during Test #4 Method B was 123.8 °C on cell #2. Thermal runaway did not propagate to any of the adjacent cells in the cell stack.

From Fig. 6a, it is interesting to note that even though the difference in time to thermal runaway between the two adjacent trigger cells are similar (~ 100 s) for both Methods A and B. Cell #5 goes into thermal runaway first in Method A whereas cell #4 goes into thermal runaway in Method B, indicating that the cell-to-cell variation results in one of the cells going into thermal runaway first. The peak temperatures of neighbors to cell #4 experience about 53 °C higher temperature during the external heating Method A (reaching close to 176 °C). Thermal runaway onset temperature is ~ 200 °C for these cells. Therefore, risk of runaway propagation is greater for Test A (External Heating). The peak temperatures on cells neighboring to the cell #5 experienced about 20 °C higher temperature during Test Method A (reaching close to 138 °C) compared to method B. The second peak is higher due to additional heat from the 1st trigger cell which is in thermal runaway and heating adjacent cells.

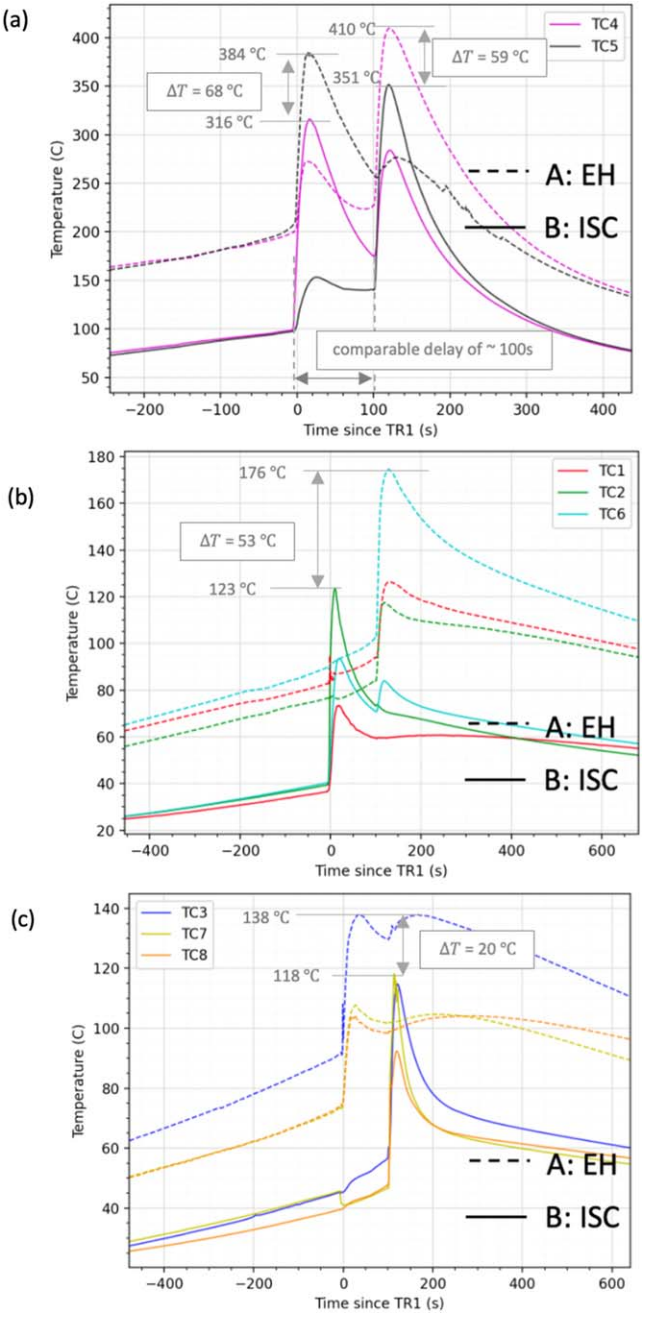

Figure 6. Comparison of thermal response from (a) cells 4 and 5 (trigger cells) (b) cell 4 neighboring (1, 2 and 6) (b) cell 5 neighboring cells (3,7 and 8).

Modeling and analysis.—These results provided motivation to further analyze the effect of the trigger mechanism on heat generation rates from various decomposition reactions. We performed a preliminary numerical analysis starting with the Arrhenius-type equations for the reactions of anode decomposition, SEI layer growth, SEI layer decomposition, cathode decomposition and the cell internal state of charge (SoC) changes.[34]

Numerical model description.—Equation 1 describes the rate of reactions between the intercalated Li-ions in the anode and the electrolyte solution to form additional SEI layers. Equation 2 describes the growth of SEI layer thickness that results from Eq. 1. Equation 3 describes the SEI layer decomposition at elevated temperatures and causing the Li-ions in SEI to react with electrolyte which is an exothermic reaction that contributes heat during the

Table II. List of model parameters used in this study.

Parameter	Description	Value	Units
ρ	Density	2580	Kg m^{-3}
cp	Specific heat capacity	830	J/kg/K
V	Cell Volume	1.663e-5	m_3
a	Surface Area	4.184e-3	m_2
A_a	Frequency Factor Anode	2.5e13	s^{-1}
A_c	Frequency Factor Cathode	6.67e11	s^{-1}
A_{ec}	Frequency Factor Short	3.37e12	s^{-1}
A_s	Frequency Factor SEI	1.67e15	s^{-1}
E_a	Activation Energy Anode	2.24e-19	J mol^{-1}
E_c	Activation Energy Cathode	2.03e-19	J mol^{-1}
E_{ec}	Activation Energy Short	1.58e-19	J mol^{-1}
E_s	Activation Energy SEI	2.24e-19	J mol^{-1}
m_a	Mass Anode	8.1e-3	kg
m_c	Mass Cathode	18.3e-3	kg
h_a	Heat Release Anode	2056e3	J kg^{-1}
h_c	Heat Release Cathode	314e3	J kg^{-1}
h_s	Heat Release SEI	257e3	J kg^{-1}
h_{ec}	Heat Release Short	5.065e3	J kg^{-1}
$x_{a,0}$	Initial Fraction of Li in anode	0.75	–
$x_{s,0}$	Initial Fraction of Li in the SEI	0.15	–
z_0	Initial dimensionless SEI thickness	0.033	–
α_0	Initial degree of conversion of cathode	0.04	–

thermal runaway process. Equation 4 describes the cathode layer decomposition where alpha is the degree of conversion of cathode material to form additional gasses. Equation 5 describes the change in SoC because of ISC device activation. Variables x_a and x_s are the amount of lithium within anode and SEI respectively. Variable z is the SEI layer thickness. The parameter values such as activation energies, frequency factors and heat releases are listed in Table II.

$$\frac{dx_a}{dt} = -x_a \cdot A_a \cdot \exp\left(-\frac{E_a}{k_b T}\right) \cdot \exp\left(-\frac{z}{z_0}\right) \quad [1]$$

$$\frac{dz}{dt} = x_a \cdot A_a \cdot \exp\left(-\frac{E_a}{k_b T}\right) \cdot \exp\left(-\frac{z}{z_0}\right) \quad [2]$$

$$\frac{dx_s}{dt} = -x_s \cdot A_s \cdot \exp\left(-\frac{E_s}{k_b T}\right) \quad [3]$$

$$\frac{d\alpha}{dt} = \alpha(1-\alpha) \cdot A_c \cdot \exp\left(-\frac{E_c}{k_b T}\right) \quad [4]$$

$$\frac{dSoC}{dt} = -ISC_{cond} \cdot SoC \cdot A_{ec} \cdot \exp\left(-\frac{E_{ec}}{k_b T}\right) \quad [5]$$

It should be noted that x_a which is the amount of lithium present in the anode that would change depending on the SoC of the Li-ion cell during internal short circuit. To account for lithium depletion in anode from electrochemical discharge during short circuit, we modify Eq. 1 as shown in Eq. 6. The constant K_{soc} relates to the amount of deintercalated lithium via electrochemical discharge process that happens with the changes in SoC, and we assumed a value of 0.7 in this investigation which is based on corresponding lithium concentration in a fully discharged cell.

$$\frac{dx_a}{dt} = -x_a \cdot A_a \cdot \exp\left(-\frac{E_a}{k_b T}\right) \cdot \exp\left(-\frac{z}{z_0}\right) + K_{soc}\frac{dSoC}{dt} \quad [6]$$

Heat generations from each decomposition reaction is given by Eqs. 7–9 whereas short circuit heat from electrochemical discharge is given by Eq. 10:

$$Q_a = m_a \cdot h_a \cdot \left| -x_a \cdot A_a \cdot \exp\left(-\frac{E_a}{k_b T}\right) \cdot \exp\left(-\frac{z}{z_0}\right) \right| \quad [7]$$

$$Q_c = m_c \cdot h_c \cdot \left| \alpha(1-\alpha) \cdot A_c \cdot \exp\left(-\frac{E_c}{k_b T}\right) \right| \quad [8]$$

$$Q_s = m_a \cdot h_s \cdot \left| -x_s \cdot A_s \cdot \exp\left(-\frac{E_s}{k_b T}\right) \right| \quad [9]$$

$$Q_{ec} = h_{ec} \cdot \left| \frac{dSoC}{dt} \right| \quad [10]$$

Analysis.—We applied the above modeling framework for the cells that have ISC device triggers (if T> 57 °C, ISCcond = 1, else ISCcond = 0) and the cells without the ISC device but triggered using the external heating (ISCcond = 0). Heat dissipation is modeled as convection and radiation with a convection coefficient of 10 $W/m^2/K$ and emissivity of 0.8. External heating is applied at 5 J s^{-1} and increasingly adjusted to ensure the temperature rate does follow the same heating rate as in our experiments which is 6 °C min^{-1} until thermal runaway occurs. We study thermal evolution for both trigger methods by applying the model to a single cell with different ambient conditions. To set the ambient temperatures appropriate for single cell and multiple cell configuration levels, we performed numerical simulation for two different ambient temperatures (T_a) of 300 K and 400 K. We assume the lower ambient conditions of 300 K are closer to single cell test conditions, and the conditions of elevated ambient temperature 400 K are closer to the multiple cell configuration test case because excess heat was absorbed by the surrounding thermal mass that eventually elevated the ambient temperatures.

Figure 7 shows the results for the lower ambient temperature case. Under these conditions, during external heating, SEI decomposition reaction is mostly completed below 420 K (Fig. 7a) which is several minutes before thermal runaway occurs (Fig. 7c). Most of this heat is lost to heat dissipation before runaway. When the ISC device is used as the trigger method, the short circuit occurs at 57 C, and initially the heat generation is dominated by Q_{ec} as can be seen in Fig. 7b. This is followed by electrochemical discharge - sei, anode and cathode decomposition reactions progress in that order within a few seconds of each other (Fig. 7c). It should also be noted that the lithium in the anode is depleted due to discharge through the short circuit resulting in less lithium available to participate in exothermic reaction at the anode after short circuit. The maximum temperature for ISC is around 33.6 K higher than that for the external heating method. Since the short circuit heats the cell in a small amount of time, decomposition reactions occur at a higher temperature. This results in higher heat generation rate due to faster kinetics. This is the cause of higher peak temperatures when using ISC devices even though overall externally supplied heat is much lower.

At higher ambient temperatures (as shown in Fig. 8), the heat dissipation from the cell is much lower. Under these conditions, the model predicts the external heating method produces a higher maximum temperature (by ∼ 23.3 K) compared to the ISC device. Most of the additional temperature can be attributed to the external heat supplied to the cell (for over 10 mins) until thermal runaway. This leads to a lower temperature peak for ISC devices even though overall heat generation (ISC + decomposition reactions) is greater.

This preliminary analysis provides several insights into the results observed during experiments. The thermal conditions during

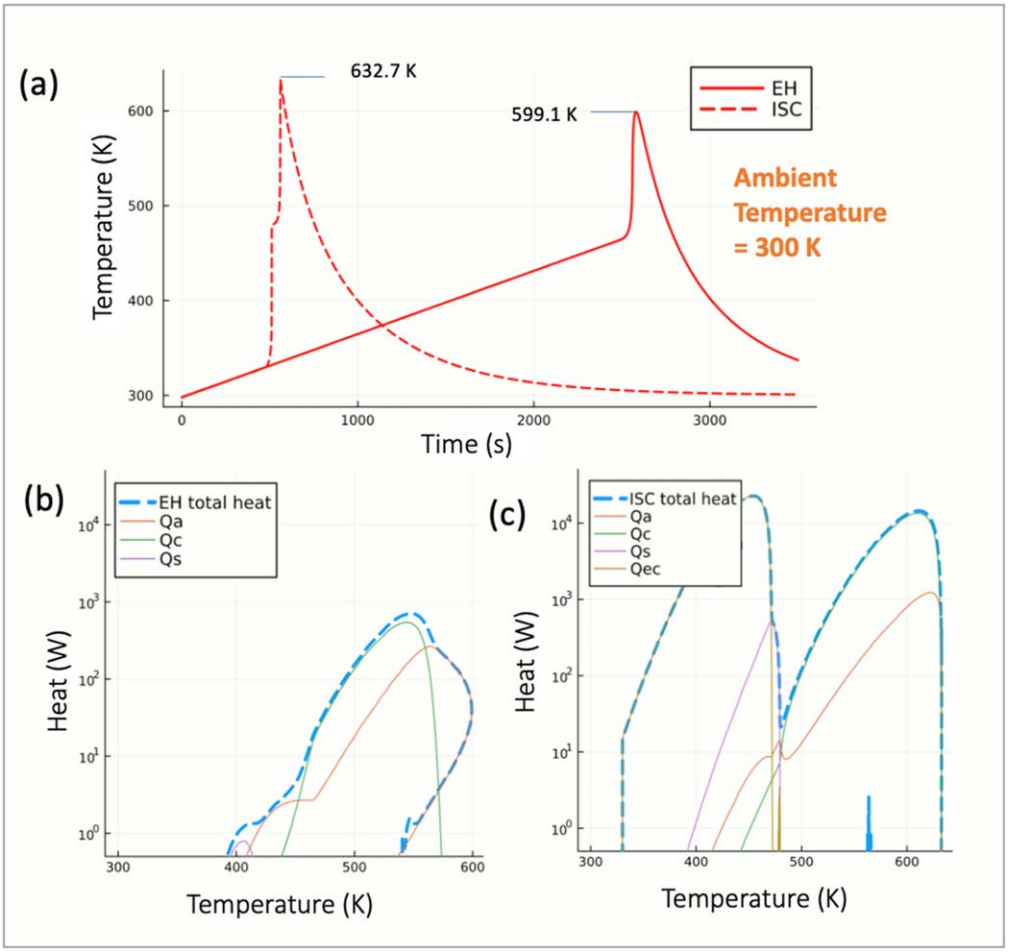

Figure 7. Thermal response of ISC trigger method vs external heating method at ambient temperature of 300 K: (a) Heat generation rate vs temperature for external heating trigger (b) Heat generation rate vs temperature for ISC trigger (c) Comparison of temperature evolution for both trigger methods.

multiple cell tests are more similar to the higher ambient temperature simulation due to heating of the additional thermal mass around the cells. This leads to lower heat dissipation compared to the single cell tests. Therefore, the experimental results presented in this study agree with the model predictions, i.e. higher peak temperatures are observed using external heating for multicell tests whereas the opposite is observed for single cell tests vs the ISC method. In this study we do not consider several factors such as loss of material from venting and combustion reactions outside the cell. Also, the parameters used are not calibrated to experimental conditions, and therefore the models do not provide quantitative prediction of thermal response. Since the temperature difference observed in neighboring cells for multicell tests is large enough to be able to determine whether cell-to-cell propagation occurs, careful analysis is required to understand which trigger method is appropriate for module level testing. Hence, well calibrated models in combination with experiments are required to improve existing safety testing methods used at module and pack level.

Conclusions

The effect of using an external film heater method to simulate internal cell short circuit and initiate thermal runaway is compared to another method where the cell is implanted with an ISC device. Both of these thermal runaway initiation methods may be used in battery pack fire safety testing. The tests are carried out at both on single cells and multiple cell configurations. In the case of single cell tests, external heating produced less severe thermal response compared to the ISC device method, whereas more severe thermal responses were observed with the external heating method in multi-cell configurations. These results indicate that the trigger method can play a significant role in the peak temperatures observed during the test as well as the possibility of cell-to-cell propagation. An ISCD implanted cell to trigger the internal short circuit is the more representative of an actual internal short circuit scenario that happens during a normal operation due to cell manufacturing process issues, material quality control issues and other such non-abuse issues. During the internal short circuits, the magnitude of short circuit current is important as it dictates the amount of heat generation which further accelerates the runaway process. The magnitude of short circuit current is significantly influenced by the battery SoC at the moment of thermal runaway initiation and cell venting, therefore determining the severity of catastrophic failure.

The work reported in this article has made critical insights on two trigger methods and how a method influences the thermal runaway process. Through comparative analysis of different failure modes at cell-level and module-level, this study shows that the severity of thermal runaway depends on interaction between internal short circuit and exothermic reactions, as well as heat transfer conditions. The outcomes of this study underscore the broader significance of selecting suitable scenarios for evaluating battery safety. Using predictive models validated against experiments is crucial to understand the battery response for a wide range of conditions such as heat transfer coefficient, state of charge and failure initiation method. Battery safety is influenced by a wide range of parameters, so it is important to understand further the influence of each parameter when planning safety test procedures. A combination of models and experiments is required to characterize battery safety in terms of abuse tolerance, severity of thermal runaway and propagation. The

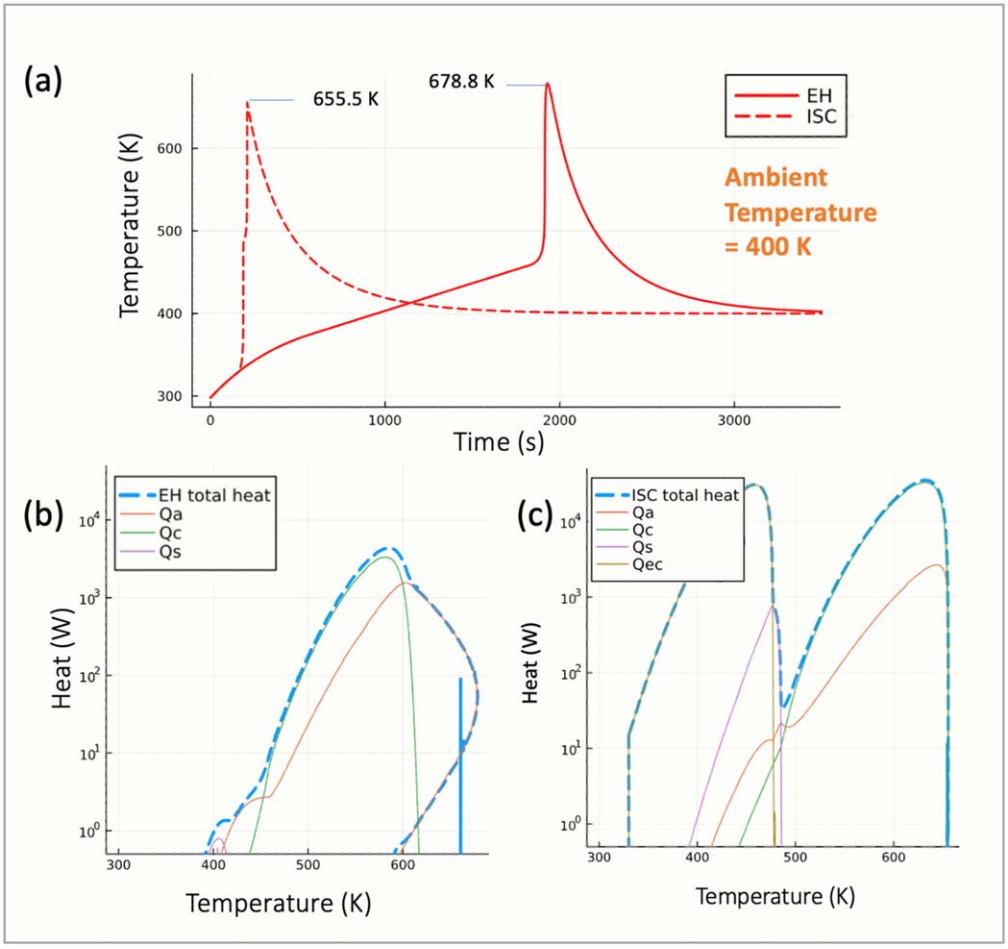

Figure 8. Thermal response of ISC trigger method vs external heating method at ambient temperature of 400 K: (a) Heat generation rate vs temperature for external heating trigger (b) Heat generation rate vs temperature for ISC trigger (c) Comparison of temperature evolution for both trigger methods.

battery safety modeling framework initiated here is a starting point for further research and development to achieve a comprehensive battery safety model and experimental test protocols.

Acknowledgments

We would like to thank Chee Chung, Engineering Director at Google LLC for the support and feedback on this technical collaboration between Google LLC and National Renewable National Laboratory.

ORCID

Anudeep Mallarapu https://orcid.org/0000-0003-3861-4748

References

1. X. Feng, M. Ouyang, X. Liu, L. Lu, Y. Xia, and X. He, "Thermal runaway mechanism of lithium ion battery for electric vehicles: a review." *Energy Storage Mater.*, **10**, 246 (2018).
2. J. Jaguemont and F. Bardé, "A critical review of lithium-ion battery safety testing and standards." *Appl. Therm. Eng.*, **231**, 121014 (2023).
3. UL 9540A, *UL Standard for Test Method for Evaluating Thermal Runaway Fire Propagation in Battery Energy Storage Systems* (2022).
4. J. Kim, A. Mallarapu, and S. Santhanagopalan, "Abuse response of batteries subjected to mechanical impact.", ed. S. Santhanagopalan *Computer Aided Engineering of Batteries* (Springer International Publishing, Cham) 199 (2023).
5. D. P. Finegan, B. Tjaden, T. M. M. Heenan, R. Jervis, M. D. Michiel, A. Rack, G. Hinds, D. J. L. Brett, and P. R. Shearing, "Tracking internal temperature and structural dynamics during nail penetration of lithium-ion cells." *J. Electrochem. Soc.*, **164**, A3285 (2017).
6. X. Zhu, H. Wang, X. Wang, Y. Gao, S. Allu, E. Cakmak, and Z. Wang, "Internal short circuit and failure mechanisms of lithium-ion pouch cells under mechanical indentation abuse conditions : An experimental study." *J. Power Sources*, **455**, 227939 (2020).
7. J. Lamb, L. Torres-Castro, J. Stanley, and C. Grosso, *ECS Meeting Abstracts*, **MA2020-01**, 104 (2020).
8. M. Zhang, J. Du, L. Liu, A. Stefanopoulou, J. Siegel, L. Lu, X. He, X. Xie, and M. Ouyang, "Internal short circuit trigger method for lithium-ion battery based on shape memory alloy." *J. Electrochem. Soc.*, **164**, A3038 (2017).
9. J. Kim, A. Mallarapu, and S. Santhanagopalan, "Transport processes in a Li-ion cell during an internal short-circuit." *J. Electrochem. Soc.*, **167**, 090554 (2020).
10. A. Mallarapu, J. Kim, K. Carney, P. DuBois, and S. Santhanagopalan, "Modeling extreme deformations in lithium ion batteries." *eTransportation*, **4**, 100065 (2020).
11. H. Li, B. Liu, D. Zhou, and C. Zhang, "Coupled mechanical–electrochemical–thermal study on the short-circuit mechanism of lithium-ion batteries under mechanical abuse." *J. Electrochem. Soc.*, **167**, 120501 (2020).
12. D. Ren, X. Feng, L. Liu, H. Hsu, L. Lu, L. Wang, X. He, and M. Ouyang, "Investigating the relationship between internal short circuit and thermal runaway of lithium-ion batteries under thermal abuse condition." *Energy Storage Mater.*, **34**, 563 (2021).
13. X. Liu et al., "Thermal runaway of lithium-ion batteries without internal short circuit." *Joule*, **2**, 2047 (2018).
14. T. D. Hatchard, D. D. MacNeil, A. Basu, and J. R. Dahn, "Thermal model of cylindrical and prismatic lithium-ion cells." *J. Electrochem. Soc.*, **148**, A755 (2001).
15. D. Ren, X. Liu, X. Feng, L. Lu, M. Ouyang, J. Li, and X. He, "Model-based thermal runaway prediction of lithium-ion batteries from kinetics analysis of cell components." *Appl. Energy*, **228**, 633 (2018).
16. J. Kim, C. Yang, J. Lamb, A. Kurzawski, J. Hewson, L. Torres-Castro, A. Mallarapu, and S. Santhanagopalan, "A comprehensive numerical and experimental study for the passive thermal management in battery modules and packs." *J. Electrochem. Soc.*, **169**, 110543 (2022).
17. M.-K. Tran, A. Mevawalla, A. Aziz, S. Panchal, Y. Xie, and M. Fowler, "A review of lithium-ion battery thermal runaway modeling and diagnosis approaches." *Processes*, **10**, 1192 (2022).
18. Q. Li, C. Yang, S. Santhanagopalan, K. Smith, J. Lamb, L. A. Steele, and L. Torres-Castro, "Numerical investigation of thermal runaway mitigation through a passive thermal management system." *J. Power Sources*, **429**, 80 (2019).

19. Y. Jia, M. Uddin, Y. Li, and J. Xu, "Thermal runaway propagation behavior within 18,650 lithium-ion battery packs: a modeling study." *Journal of Energy Storage*, **31**, 101668 (2020).
20. A. Misar, A. Jain, J. Xu, and M. Uddin, "Development of a computational fluid dynamics simulation framework for aerothermal analyses of electric vehicle battery packs." *Journal of Electrochemical Energy Conversion and Storage*, **21**, 031009 (2024).
21. G.-H. Kim, A. Pesaran, and R. Spotnitz, "A three-dimensional thermal abuse model for lithium-ion cells." *J. Power Sources*, **170**, 476 (2007).
22. X. Feng, X. He, M. Ouyang, L. Wang, L. Lu, D. Ren, and S. Santhanagopalan, "A coupled electrochemical-thermal failure model for predicting the thermal runaway behavior of lithium-ion batteries." *J. Electrochem. Soc.*, **165**, A3748 (2018).
23. H. Li, D. Zhou, M. Zhang, B. Liu, and C. Zhang, "Multi-field interpretation of internal short circuit and thermal runaway behavior for lithium-ion batteries under mechanical abuse." *Energy*, **263**, 126027 (2023).
24. X. Duan, H. Wang, Y. Jia, L. Wang, B. Liu, and J. Xu, "A multiphysics understanding of internal short circuit mechanisms in lithium-ion batteries upon mechanical stress abuse." *Energy Storage Mater.*, **45**, 667 (2022).
25. Y. Jia, X. Gao, L. Ma, and J. Xu, "Comprehensive battery safety risk evaluation: aged cells versus fresh cells upon mechanical abusive loadings." *Adv. Energy Mater.*, **13**, 2300368 (2023).
26. B. Liu, Y. Jia, J. Li, S. Yin, C. Yuan, Z. Hu, L. Wang, Y. Li, and J. Xu, "Safety issues caused by internal short circuits in lithium-ion batteries." *J. Mater. Chem. A*, **6**, 21475 (2018).
27. D. Zhou, H. Li, Z. Li, and C. Zhang, "Toward the performance evolution of lithium-ion battery upon impact loading." *Electrochim. Acta*, **432**, 141192 (2022).
28. H. Li, D. Zhou, J. Cao, Z. Li, and C. Zhang, "On the damage and performance degradation of multifunctional sandwich structure embedded with lithium-ion batteries under impact loading." *J. Power Sources*, **581**, 233509 (2023).
29. J. Kim, A. Mallarapu, D. P. Finegan, and S. Santhanagopalan, "Modeling cell venting and gas-phase reactions in 18650 lithium ion batteries during thermal runaway." *J. Power Sources*, **489**, 229496 (2021).
30. J. K. Ostanek, W. Li, P. P. Mukherjee, K. R. Crompton, and C. Hacker, "Simulating onset and evolution of thermal runaway in Li-ion cells using a coupled thermal and venting model." *Appl. Energy*, **268**, 114972 (2020).
31. M. Keyser, E. Darcy, D. Long, and A. Pesaran, *US Patent*, US9142829B2 (2015).
32. D. P. Finegan et al., "Characterising thermal runaway within lithium-ion cells by inducing and monitoring internal short circuits." *Energy Environ. Sci.*, **10**, 1377 (2017).
33. J. Lamb, L. Torres-Castro, J. C. Hewson, R. C. Shurtz, and Y. Preger, "Investigating the role of energy density in thermal runaway of lithium-ion batteries with accelerating rate calorimetry." *J. Electrochem. Soc.*, **168**, 060516 (2021).
34. P. T. Coman, E. C. Darcy, C. T. Veje, and R. E. White, "Modelling Li-Ion cell thermal runaway triggered by an internal short circuit device using an efficiency factor and arrhenius formulations." *J. Electrochem. Soc.*, **164**, A587 (2017).